Mineralogical Magazine (2021), **85**, 484–495
doi:10.1180/mgm.2020.97

CAMBRIDGE
UNIVERSITY PRESS

Article – Gregory Yu. Ivanyuk memorial issue

Mineralogy of volcanic calciocarbonatites from the Trig Point Hill debris flow, Kerimasi volcano, Tanzania: implications for the altered natrocarbonatite hypothesis

Roger H. Mitchell[1]* and J. Barry Dawson[2],†

[1]Department of Geology, Lakehead University, Thunder Bay, Ontario, Canada P7B 5E1; and [2]School of Geosciences, Grant Institute, University of Edinburgh, King's Buildings, Edinburgh, Scotland, UK EH9 3FE

Abstract

A major debris flow, the Trig Point Hill flow, originating from Kerimasi volcano (Tanzania) contains numerous blocks of extrusive/pyroclastic carbonatites similar to those exposed at the rim of the currently inactive crater. The blocks of calcite carbonatite consist of: (1) large clasts of corroded and altered coarse grained calcite; (2) primary prismatic inclusion bearing phenocrystal calcite; and (3) a matrix consisting primarily of fine-grained prismatic calcite. The large clasts are inclusion free and exhibit a 'corduroy-like' texture resulting from solution along cleavage planes. The resulting voids are filled by brown Fe–Mn hydroxides/oxides and secondary calcite. The prismatic or lath-shaped phenocrystal calcite is not altered and contains melt inclusions consisting principally of primary Na–Ca carbonates which contain earlier-formed crystals of monticellite, periclase, apatite, Mn–Mg-magnetite, Mn–Fe-sphalerite and Nb-perovskite. Individual Na–Ca carbonate inclusions are of uniform composition, and the overall range of all inclusions analysed (wt.%) is from 28.7 to 35.9 CaO; 16.7–23.6 Na_2O; 0.5–2.8 K_2O, with minor SO_3 (1.1–2.2) and SrO (0.34–1.0). The Na–Ca carbonate compositions are similar to that of shortite, although this phase is not present. The Na–Ca carbonates are considered to be primary deuteric phases and not secondary minerals formed after nyerereite. Monticellite shows limited compositional variation and contains 2–4 wt.% MnO and 12 wt.% FeO and is Mn-poor relative to monticellite in Oldoinyo Lengai natrocarbonatite. Periclase is Fe-bearing with up to 13 wt.% FeO. Spinels are Cr-free, Mn-poor and belong to the magnetite–magnesioferrite series in contrast to Mn-rich spinels of the magnetite–jacobsite series occurring in Oldoinyo Lengai natrocarbonatite. The matrix in which the 'corduroy' clasts and phenocrystal calcite are set consists of closely packed small prisms of calcite lacking melt inclusions, with interstitial fine-grained apatite, baryte, strontianite and minor fluorite. Pore spaces are filled with secondary Mn–Fe hydroxides/oxides, anhydrite and gypsum. The hypothesis that flow-aligned calcite in volcanic calciocarbonatites from Kerimasi, Tinderet, Homa and Catanda is altered nyerereite is discussed and it is considered that these calcite are either primary phases or altered melilite. The nyerereite alteration hypothesis is discussed with respect to the volumetric and compositional aspects of pseudomorphism by dissolution–precipitation replacement mechanisms. This study concludes that none of the volcanic calciocarbonatites containing flow-aligned calcite phenocrysts are altered natrocarbonatite.

Keywords: carbonatite, natrocarbonatite, nyerereite, alkali carbonate, monticellite, jacobsite, magnesioferrite, Kerimasi, Tinderet, Oldoinyo Lengai

(Received 10 September 2020; accepted 23 November 2020; Accepted Manuscript published online: 27 November 2020;
Guest Editor: Anatoly Zaitsev)

Introduction

Kerimasi (2°51'S, 35°5'E) is a dormant stratovolcano located in the Gregory Rift Valley of northern Tanzania and in common with the adjacent active Oldoinyo Lengai volcano (2°75'S, 35° 90'E), belongs to the series of younger volcanoes (<1.2 Ma) of the Neogene-to-Recent volcanic field of the North Tanzania Divergence of the East African Rift System (Dawson, 2008). Oldoinyo Lengai is the only known volcano to erupt natrocarbonatites. These consist principally of nyerereite, gregoryite, sylvite–halite solid solutions and fluorite. The paucity of fresh natrocarbonatites in the geological record has given rise to the hypothesis that other nephelinite–carbonatite volcanoes (e.g. Fort Portal, Uganda; Homa Mountain, Kenya; Tinderet, Kenya; Catanda, Angola) also erupted natrocarbonatites and that nyerereite in these lavas has been altered to flow-aligned calcite during subaerial weathering (Hay, 1983; Deans and Roberts, 1984; Clarke and Roberts, 1986; Zaitsev *et al.*, 2008; Zaitsev, 2010). The concept originated from a belief that calcite could not crystallise at atmospheric pressure from a carbonatitic magma; an idea which was shown subsequently to be incorrect by the experimental studies of haplocarbonatites by Gittins and Jago (1991). The hypothesis has been questioned by: Le Bas (1984); Bailey (1993); Gittins and Jago (1991); Gittins and Harmer (1997); and Woolley and Church (2005).

***Author for correspondence:** Roger H. Mitchell, Email: rmitchel@lakeheadu.ca

†Deceased, 1932–2013

This paper is part of a thematic set 'Alkaline Rocks' in memory of Dr Gregory Yu. Ivanyuk

Cite this article: Mitchell R.H. and Dawson J.B. (2021) Mineralogy of volcanic calciocarbonatites from the Trig Point Hill debris flow, Kerimasi volcano, Tanzania: implications for the altered natrocarbonatite hypothesis. *Mineralogical Magazine* **85**, 484–495. https://doi.org/10.1180/mgm.2020.97

The comprehensive investigations by Dawson *et al.* (1987), Keller and Zaitsev (2006), Zaitsev and Keller (2006) and Zaitsev *et al.* (2008, 2009) showed conclusively that natrocarbonatites alter initially to pirssonite plus gaylussite and ultimately to calcite with, in some instances, preservation of natrocarbonatite textural features. However, the applicability of these observations in general to eruptive calciocarbonatites with flow-aligned calcite remains debatable. The Oldoinyo Lengai calcite-rich altered natrocarbonatites were termed ‘calcite carbonatite’ by Zaitsev and Keller (2006) and Zaitsev *et al.* (2008), albeit with proviso that the calcite in these rocks is not of primary magmatic origin. Unfortunately, this terminology is inappropriate and misleading, and it is suggested here that ‘calcareous carbonatite’ is perhaps a better description of these rocks which avoids any confusion with primary calcite carbonatites.

In the search for altered natrocarbonatites Kerimasi and Tinderet have played key roles. Kerimasi is a dormant nephelinite volcano which has preserved erupted calcite carbonatite tephra and lava at the crater rim and diverse calcite carbonatites within the pyroclastic sequence (Guest, 1953; Mariano and Roeder, 1983; Church, 1995). Many of these rocks have been interpreted to be altered natrocarbonatites and it was Hay’s (1983) descriptions of flow-aligned calcite carbonatites from Trig Point Hill on the south-eastern flank of Kerimasi, which instigated the altered natrocarbonatite controversy.

The Kerimasi pyroclastics also contain many plutonic xenoliths ranging from afrikandite through ijolite series rocks to coarse-grained primary calcite carbonatites (Church, 1995; Dawson, 2008; Zaitsev 2010; Guzmics *et al.*, 2011). There are major differences between Kerimasi and Oldoinyo Lengai in that the latter has erupted diverse peralkaline phonolites and lacks both primary plutonic or eruptive calcite carbonatites. Hence, direct comparisons between the two volcanoes might not be appropriate as, although in geographical proximity, their petrology is clearly different (Dawson, 2008). Kerimasi actually has greater petrological affinities with the melilitite/nephelinite magmatism of the Natron–Engaruka tuff cone area (Dawson, 2008; Mattsson, 2012) than with Oldoinyo Lengai.

With regard to Tinderet, the influential paper of Deans and Roberts (1984), appears to have established the ‘altered nyerereite’ hypothesis as received wisdom, with this being perpetuated by: Clarke and Roberts (1986) for Homa Mountain (Kenya); Zaitsev *et al.* (2013) for Tinderet; and Campeny *et al.* (2015) for Catanda (Angola). Unfortunately, the Deans and Roberts (1984) paper appears to contain a major error in that the caption for figure 3b (p. 568) refers to the rock illustrated (p. 569) as a natrocarbonatite from Oldoinyo Lengai. However, the text (p. 568, l.1-9) refers to this figure as illustrating textural features of a Tinderet sample. Figure 3b, actually shows none of the textural features of either fresh (Peterson, 1990; Keller and Krafft, 1990) or altered Oldoinyo Lengai natrocarbonatite (Zaitsev *et al.*, 2008), and in keeping with all other sub-figures in figure 3 of Deans and Roberts (1984) must be a Tinderet sample. This observation is discussed further below.

This work presents data for carbonatite lavas preserved in a major debris flow originating from sector collapse of the southeast flank of Kerimasi volcano (Fig. 1). Samples were collected from Trig Point Hill, a region referred to as site 6 by Hay (1983). These data have a direct bearing on the problem of the absence of natrocarbonatites in general, as we show that these lavas cannot be altered natrocarbonatite as suggested by the previous studies of Hay (1983); a conclusion that is also applicable to similar rocks occurring at the Tinderet and Homa volcanoes (Deans and Roberts, 1984; Clarke and Roberts, 1986; Zaitsev *et al.*, 2013) and Catanga (Campeny *et al.*, 2015). This contribution by addressing mineralogical and petrographic data, together with solution/deposition models of pseudomorphism, demonstrates that the hypothesis that flow-aligned calcite crystals in some calciocarbonatites are pseudomorphs after nyerereite is not correct.

Kerimasi debris flow

The major avalanche deposit formed by collapse of the south-eastern flank of Kerimasi (Fig. 1) has been described by Hay (1983), Kervyn *et al.* (2008) and Delcamp *et al.* (2016). This deposit extends from a scarp at an elevation of ~2000 m approximately 8.9 km in a south-easterly direction to the surrounding Engaruku Basin plains (~800 m). The flow covers an area of ~33 km^2 and has an average thickness of 30 m. The distal lobe is ~8 m in thickness at a location known locally as Trig Point Hill. The debris flow did not originate at the summit of Kerimasi and thus does not include any of the crater rim carbonatites. Although the debris flow has not been investigated in any detail it consists of a heterogeneous assemblage of a matrix of finely comminuted pyroclastic nephelinite and carbonatite with large blocks of carbonatite together with a wide assortment of coarse grained clasts (1–20 cm) of diverse ijolite series rocks and melilite-bearing rocks (afrikandite; uncomphagrite) plus xenocrysts of clinopyroxene, titanite and garnet. This plutonic suite is a microcosm of the petrology of the substructure of the volcano, which has not as yet been thoroughly investigated, although some mineralogical data for an afrikandite are given by Guzmics *et al.* (2012).

Trig Point Hill carbonatites

The debris flow at its distal lobe contains a distinctive assemblage of large blocks of carbonatite tephra (Fig. 2) including a distinct variety of clast (~3 cm × 1 cm) dominated by a macroscopic texture referred to as ‘corduroy’ calcite. This texture appears to result from the development of solution spaces (<0.2–0.35 mm) along the cleavage planes of closely-spaced (0.2–0.4 mm) parallel calcite lamellae. The voids created are, in part or in whole, filled with amorphous brown Fe–Mn hydroxide/oxides and microcrystalline calcite (Fig. 2a,d). Similar ‘corduroy’ calcite carbonatite has been recognised by Church (1995) and Zaitsev (2010) from the north-eastern slopes of the volcano and, by the authors of this study, at the crater rim.

Three morphological types of calcite (Figs 2) are present in the carbonatite tephra: ‘corduroy’ calcite (C1); primary resorbed prismatic (0.5–2 mm) inclusion-bearing ‘phenocrystal’ calcite (C2); fine grained (<1 mm), flow-aligned prismatic calcite (C3). The ‘phenocrystal’ calcite (C2) in many instances contains inclusions of 1–100 μm multi-phase ovoid melt inclusions containing: Na–Ca carbonates; subhedral compositionally-zoned monticellite; periclase; Mn-Mg magnetite; Mn–Fe-sphalerite and Nb-perovskite.

The matrix in which the ‘corduroy’ calcite clasts (C1) and phenocrystal (C2) calcite are set consists of closely-packed, flow-aligned, small stubby prisms of calcite (C3) lacking melt inclusions together with interstitial fine-grained apatite, baryte, strontianite, trace fluorite and xenocrystal clinopyroxene, titanite and Ti andradite (Fig. 3). Pore spaces are filled with secondary Mn-oxides/hydroxides, anhydrite and gypsum.

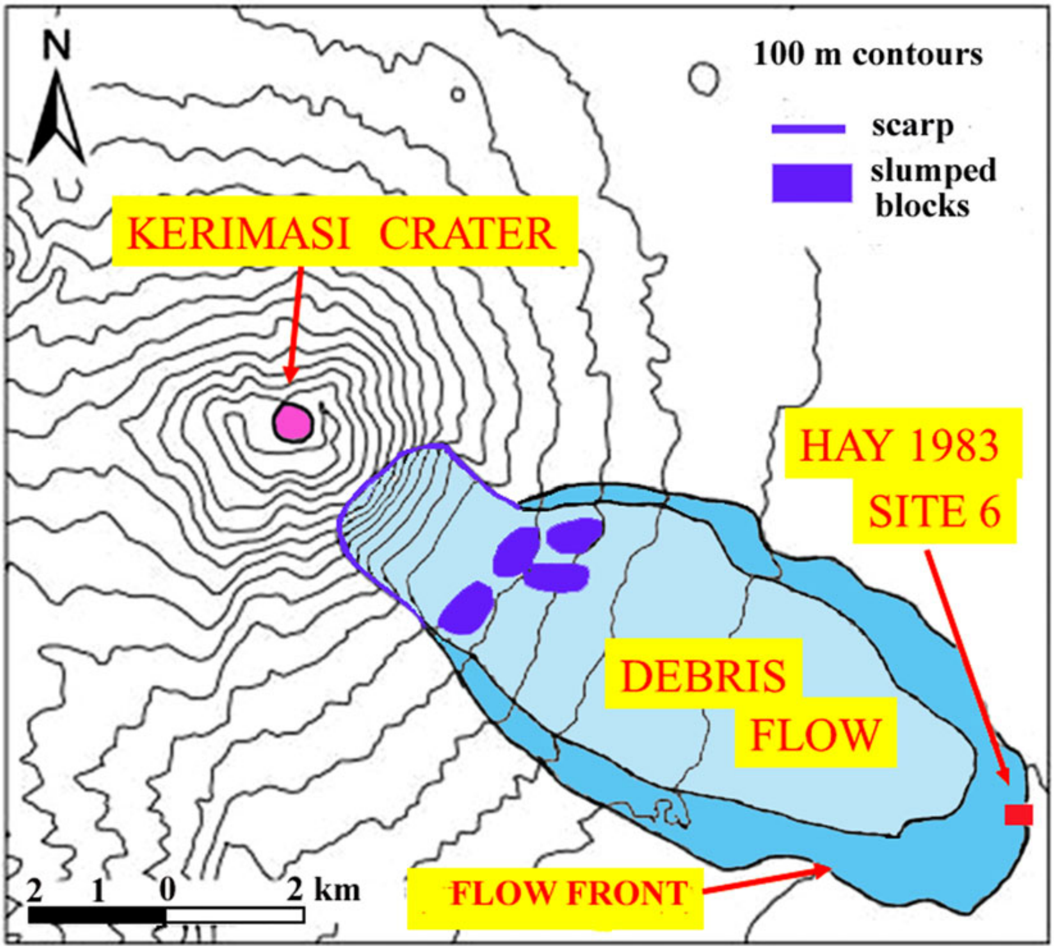

Fig. 1. Topographic map of Kerimasi volcano (after Kervyn *et al.*, 2008) showing the location of the currently inactive crater and the debris flow formed by sector collapse. The termination of the debris flow at Trig Point Hill is the locality #6 originally investigated by Hay (1983).

Analytical methods

Polished thin sections, prepared in kerosene, were examined by standard petrographic methods and back-scattered electron petrography. Compositions of the phases present were determined by quantitative energy dispersive X-ray spectrometry using a Hitachi FE-SU70 scanning electron microscope equipped with the Oxford Instruments AZtec software package. The electron accelerating voltage was 20 kV and beam current 300 pA. Standards used were: synthetic pyroxene glass (Si, Ca); corundum (Al); jadeite (Na,Al); CaF_2 (Ca, F) Mn-hortonolite (Mg, Fe, Si, Mn); ilmenite (Ti, Fe); synthetic rare element phosphates (Ca, La, Ce, Pr, Nd, Sm, P); $SrTiO_3$ (Sr, Ti), $BaSO_4$ (Ba, S); and $ThNb_2O_{12}$ (Nb).

The analysis of the Na–Ca carbonates present in the melt inclusions proved to be challenging as they have quenched to a porous aggregate of extremely fine-grained microcrystals rather than a glass. The use of rastered small areas (10 μm^2) and the low beam currents (300 pA) employed for analysis permitted reproducible analyses of these carbonatites. During analysis the X-ray count-rate for Na did not decrease and there was no obvious decomposition of the samples. However, given the presence of the micro-voids in the quench aggregates, it is considered that the compositions determined represent those of carbonate plus micro-voids. Thus, the reported compositions (Table 4) include this contribution which, on the basis of secondary electron imagery and estimation of CO_2 content, is estimated to be small but not constant. The Na, Ca and K contents are considered to be accurate and any calculated equivalent carbonate based on these data indicates the amount of void contribution and does not reflect analytical error. Hence, it is considered that the reported compositions are realistic for the purposes of this study

Mineral compositions

Calcite

All three textural varieties of calcite contain <0.2 wt.% FeO and MnO, and have very limited compositional variation with respect to Sr and Mg (Table 1). Only the ‘corduroy’ calcite (C1) contains minor amounts of MgO ranging from <0.2–0.6 wt.%. Their SrO contents are low (<0.2–0.5 wt.%) relative to prismatic (C2) and lath (C3) calcite, which are similar with SrO ranging from 0.5–0.9 wt.% (Table 1). Individual crystals of ‘corduroy’ calcite do not exhibit any significant compositional variation within and between parallel lamellae, and individual crystals of lath (C3) calcite are homogeneous. Prismatic (C2) calcite in some crystals exhibits weak heterogeneous irregular zoning with respect to SrO (0.5–0.9 wt.%), a range identical to that determined for this calcite paragenesis as a whole. The above SrO contents are similar to those reported by Zaitsev (2010) for single crystals (0.73–0.78 wt.%; C2 in this work) and banded calcite (0.1–0.54 wt.%; C1 in this work).

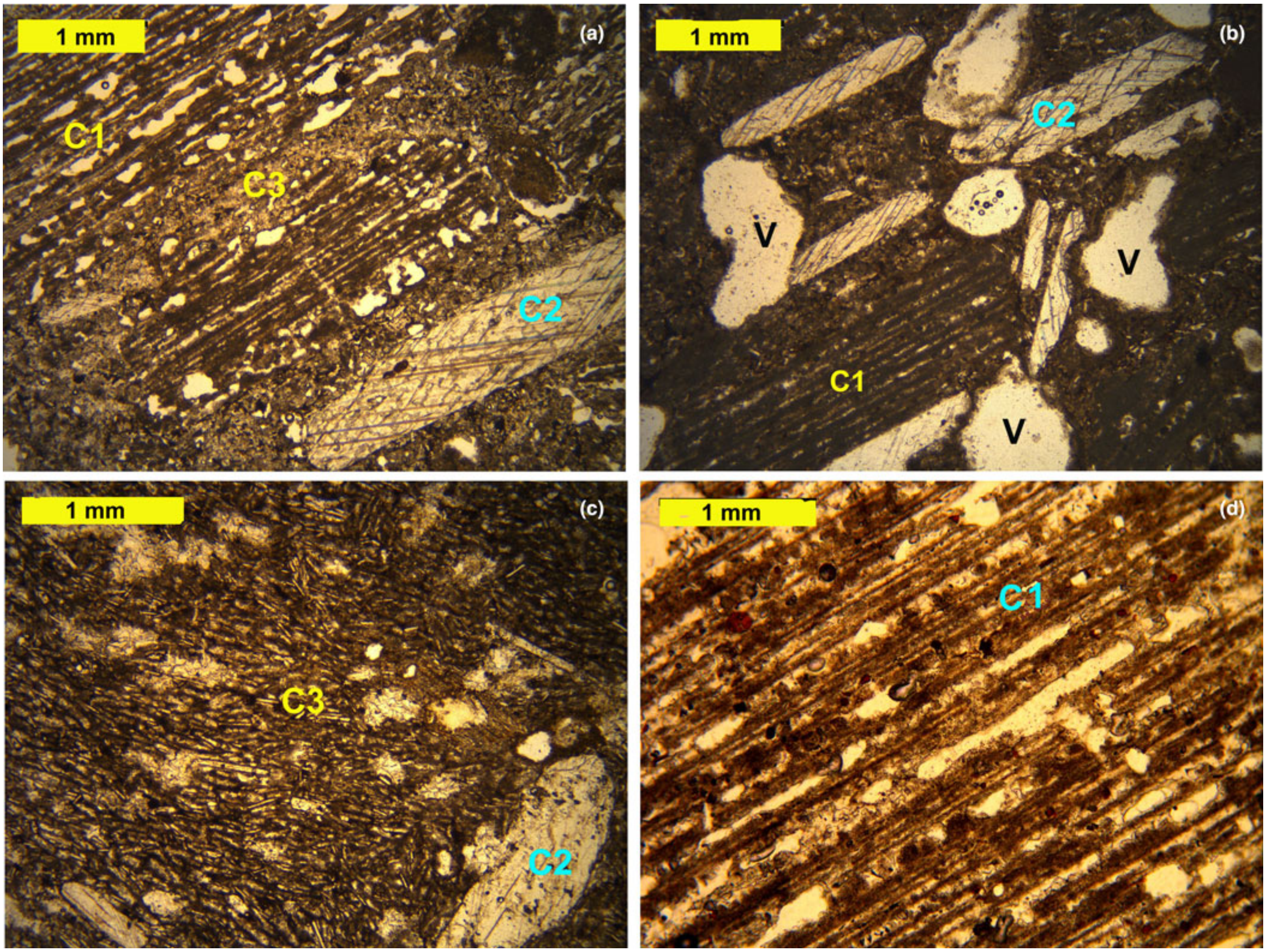

Fig. 2. Transmitted light photomicrographs of Trig Point Hill carbonatites illustrating the heterogeneous texture and the three varieties of calcite. (a) corduroy calcite (C1) and prismatic calcite (C2) set in the very fine grained matrix of calcite laths (C3); (b) Corduroy calcite (C1) and flow-aligned, resorbed prismatic calcite (C2), V = voids; (c) the matrix of the breccia consisting of fine grained flow-aligned prismatic calcite (C3); and (d) texture of corduroy calcite (C1) illustrating parallel bands of replacement plus voids of colourless calcite and brown bands of amorphous Mn–Fe hydroxide/oxides plus calcite.

Monticellite

Monticellite occurs as euhedral-to-subhedral microphenocrysts in calcite (C2) laths or less commonly in melt inclusions with apatite and Na–Ca carbonate (Fig. 4). It exhibits a very limited compositional range in MnO (2.3–4.1 wt.%) at near-constant FeO (1.3–1.8 wt.%) content. (Table 2). The principal substitution is within the monticellite–glaucochroite series ($Mo_{87-93}Glc_{3.8-9.3}Kir_{2.8-4.9}$ mol.%); (Mo = $CaMgSiO_4$; Glc = $CaMnSiO_4$; Kir = $CaFeSiO_4$). The monticellite is of identical composition to that in Kerimasi plutonic calcite carbonatite (Fig. 5) reported by Guzmics *et al.* (2011), but differs substantially from the manganoan monticellite in Oldoinyo natrocarbonatites (Fig. 5) described by Mitchell and Belton (2004; 2008). This difference in Mn content is significant with respect to the hypothesis that these tephra are altered natrocarbonatites (see below).

Apatite

Apatite is scattered throughout the matrix of the prismatic lath calcite (C3) as rare anhedral small (<20 µm) crystals commonly in association with Mn–Fe hydroxide/oxides, baryte, celestite, anhydrite, gypsum and spinels (Fig. 3).The apatite is of near-stoichiometric composition, with REE and Mn not detectable by EDS methods (<0.2 wt.%), and containing 2.1–2.9 wt.% SiO_2, 0.6–0.9 wt.% SrO, and 1.6–3 wt.% F.

Apatite is notably absent as single crystal inclusions in prismatic (C2) calcite and occurs only in melt inclusions as rounded-to-lobate resorbed small crystals (<20 µm) in association with Na–Ca carbonates, periclase and Nb-perovskites (Fig. 4). In common with apatite associated with calcite (C3) these apatites have low contents (wt.%) of SrO (0.42–0.55), SiO_2 (2–3) and F (1.1–3.5). The paucity of primary phenocrystal apatite relative to its abundance in Kerimasi crater rim carbonatite (see below) is a significant difference to the Trig Point Hill carbonatites.

Spinels

Spinels occur principally as small (<25 µm) anhedral-to-subhedral crystals in the interstices between prismatic calcite (C3) in association with apatite, Mn–Fe hydroxides/oxides, celestite, anhydrite and gypsum. Spinels are rarely present as very small (<5 µm) anhedral crystals in Na–Ca carbonate-bearing

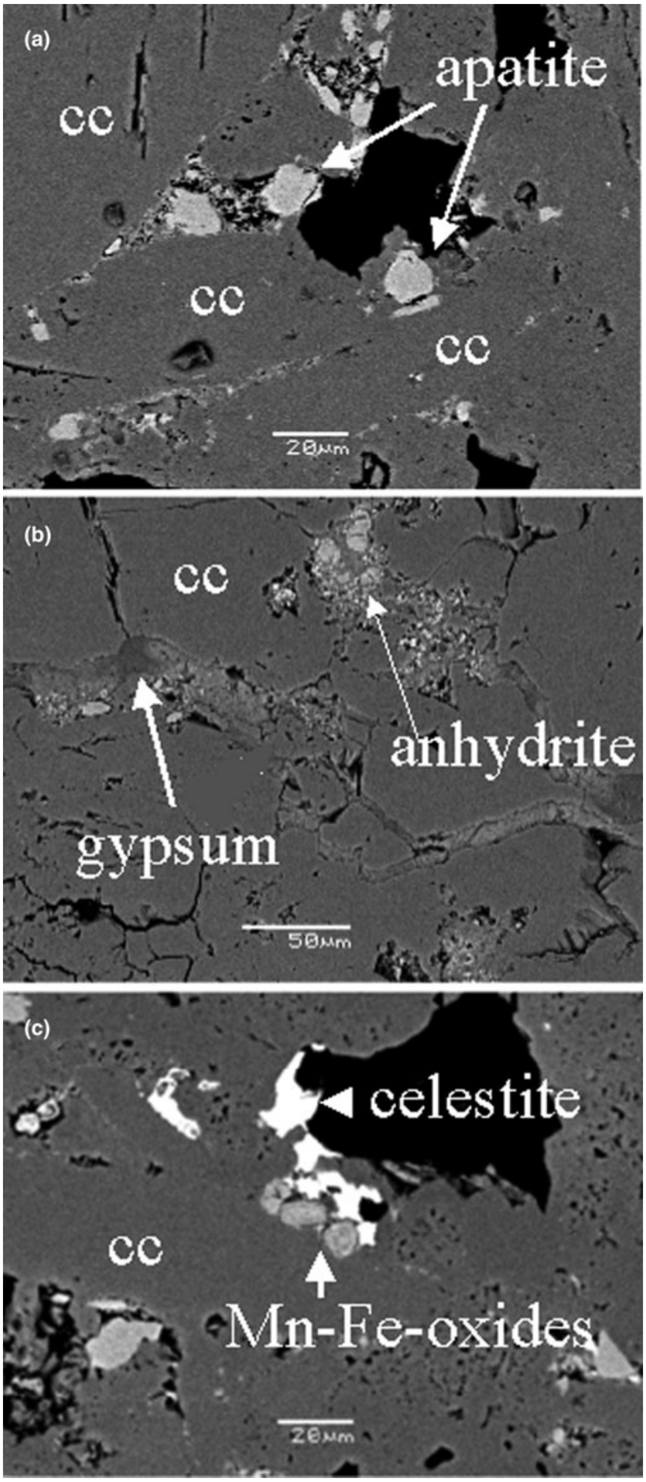

Fig. 3. Back-scattered electron images of the matrix of the Trig Point Hill breccia. (a) Calcite laths (cc) with interstitial anhedral apatite and voids (black); (b) interstitial gypsum and anhydrite; and (c) interstitial Mn–Fe hydroxide/oxides, celestite and voids.

Table 1. Representative compositions of calcite.

Wt.%	1	2	3	4	5	6	7	8	9
MgO	0.32	0.37	0.62	n.d.	n.d.	n.d.	n.d.	n.d.	n.d
CaO	55.40	54.87	54.43	55.25	54.90	54.89	55.31	54.86	54.87
SrO	n.d.	0.49	0.16	0.44	0.78	0.94	0.69	0.83	0.94
Σ	55.72	55.73	55.21	55.69	55.68	55.83	56.00	55.69	55.91
Wt.% carbonate									
$MgCO_3$	0.67	0.77	1.30						
$CaCO_3$	98.88	97.93	97.15	98.61	97.99	97.97	98.72	97.91	97.93
$SrCO_3$		0.70	0.23	0.63	1.11	1.34	0.98	1.18	1.37
Σ	99.55	99.40	98.67	99.24	99.10	99.31	99.70	99.10	99.30
Mol.% carbonate									
$MgCO_3$	0.80	0.93	1.56						
$CaCO_3$	99.20	98.59	98.28	99.57	99.24	99.08	99.33	99.19	99.06
$SrCO_3$		0.48	0.16	0.43	0.76	0.92	0.67	0.81	0.94

Compositions: 1–3 courdoy calcite (C1); microphenocrystal calcite (C2); 6–9 fine grained prismatic calcite (C3). n.d. = not detected (<0.15% oxide).

melt inclusions in calcite (2), and are absent in corduroy calcite (C1).

Spinels exhibit a very wide range in composition (Table 3; Fig. 6) and are essentially members of the magnesioferrite–jacobsite–ulvöspinel–magnetite solid-solution series. The crystals are too small to establish any zonation trends, although increased Mn contents of individual crystals are correlated with decreasing Ti contents.

Apatite calcite carbonatite and tephra are exposed at the crater rim at Kerimasi (Mariano and Roeder, 1983, this work). The tephra are similar in their petrography to the Trig Point Hill carbonatites in containing calcite similar to the corduroy (C1) and prismatic (C2) calcite. The coarse-grained apatite carbonatites contain subhedral-to-anhedral (20–100 µm) spinels in close association with apatite. The apatite is commonly rounded and contains melt inclusions dominated by Na–Ca-carbonate. The spinels, in common with Trig Point Hill spinels, are members of the magnesioferrite–jacobsite–ulvöspinel–magnetite solid solution and exhibit a limited range in composition (Table 3; Fig. 6). Some compositions are similar to spinel compositions reported by Reguir *et al.* (2008) from a Kerimasi north slope calcite carbonatite, although the majority of these spinels are richer in magnetite (Fig. 6). In contrast to Trig Point Hill, spinels in other carbonatites from the north slopes of Kerimasi (this work; Guzmics *et al.*, 2011), occur in abundance as large euhedral crystals within apatite veins (Fig. 7a) and Na–Ca-carbonate inclusions. (Fig. 7b).

In summary, all spinel compositions from diverse Kerimasi calcite carbonatites are Mn-poor relative to Mn-rich spinels occurring in fresh and altered Oldoinyo Lengai natrocarbonatites (Mitchell and Belton, 2004, 2008; Keller and Zaitsev, 2006; Fig. 6); an observation indicating that the Trig Point Hill carbonatites are unlikely to be altered natrocarbonatite.

Periclase

Small crystals of periclase (<20 µm) occur as inclusions in, or at the margins, of monticellite inclusions in calcite (C2), and rarely as small crystals (<10 µm) in Na–Ca carbonate inclusions. (Fig. 4a,b). These relations indicate that periclase is a primary liquidus phase. There is no petrographic or mineralogical evidence to indicate its presence in this carbonatite results from decarbonation of dolomite as suggested by Treiman and Essene (1984) for periclase occurring at the Oka complex or by decarbonation to produce calcite and periclase with further reaction to produce forsterite, monticellite, garnet and melilite as suggested by Stoppa *et al.* (2019) for some Italian carbonatites.

The compositions (wt.%) of two crystals large enough for analysis without excitation of their host monticellite are: (1) 84.54 MgO; 13.33 FeO_T; 2.62 MnO; and (2) 85.47 MgO; 13.30 FeO_T;

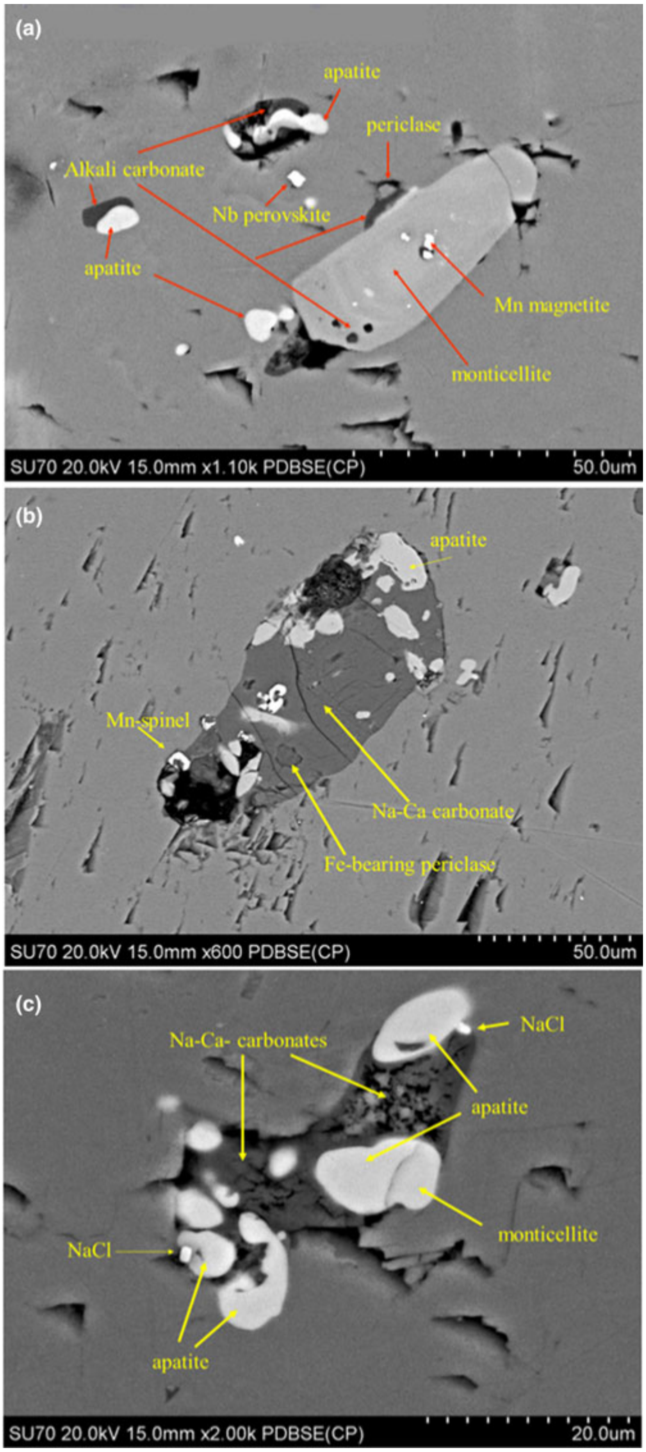

Fig. 4. Back-scattered electron images of inclusions in Trig Point Hill prismatic calcite (C2). (a) Large monticellite inclusion with Na–Ca carbonate and Mn-magnetite inclusions associated with periclase. Also shown are round melt inclusions consisting principally of Na–Ca carbonate and resorbed apatite; (b) Na–Ca carbonate inclusion with resorbed apatite, periclase and Mn-magnetite; and (c) Na–Ca carbonate inclusion with resorbed apatite, monticellite and NaCl.

2.48 MnO. These correspond respectively to $(Mg_{0.90}Fe_{0.08}Mn_{0.02})O$ and $(Mg_{0.906}Fe_{0.079}Mn_{0.015})O$, indicating these are ferro-periclase with a significant Mn content. Similar, but more abundant, ferro-periclase (wt.%: 84.3 MgO; 12.6 FeO_T; 1.8 MnO) coexisting with monticellite has been reported by Mariano and Roedder (1983) from an apatite–periclase calcite carbonatite occurring in the centre of the Kerimasi crater.

Na–Ca carbonate

Calcite (C2) contains numerous oval-to-lobate multi-phase melt inclusions ranging in size from <10–150 µm. They are characterised primarily by the presence of apatite set in a matrix of Na–Ca carbonate (Fig. 4). Inclusions containing approximately equal amounts of apatite and carbonate are common. Apatite in the inclusions always occurs as rounded crystals which in some instances exhibit resorbed embayed margins. Less common minerals, typically <5 vol.%, occurring as single crystals (<10 µm), included in the carbonates, in order of decreasing frequency of occurrence are: euhedral monticellite; latrappite; perovskite; magnesioferrite; periclase; Mn-sphalerite; and very rare halite. Representative compositions of the Na–Ca carbonates are given in Table 4. Individual inclusions contain carbonates of uniform composition, although the overall range of all inclusions analysed (wt.%) is from 28.7 to 35.9 CaO; 16.7–23.6 Na_2O; 0.5–2.8 K_2O, with minor SO_3 (1.1–2.2) and SrO (0.34–1.0). The compositional variation is illustrated in Fig. 8 and shows a poor anti-correlation between CaO and (Na+K) contents. Compositions are closer to shortite $[Na_2Ca_2(CO_3)_3]$ rather than nyerereite $[Na_2Ca(CO_3)_2]$.

The composition of Na–Ca-carbonates hosted by melt inclusions in Kerimasi calcite carbonate (this work) are also shown on Fig. 8. These carbonates are essentially identical to those from Trig Point Hill. The inclusions are also characterised by rounded resorbed apatite but differ in containing more spinel (Fig. 7). Na–Ca carbonates occurring in association with silicates are common in magnetite and perovskite in melt inclusions from Kerimasi afrikandite (this work; Guzmics *et al.*, 2012). These are, in contrast, relatively poor in Ca and show a limited range in CaO (26.1–27.90 wt.%), with a wide range in Na_2O (17.8–22.5 wt.%) and ($Na_2O + K_2O$; 23.1–28.5 wt.%) together with significant K_2O (5.2–6.5 wt.%) contents. The compositional variation in terms of CaO versus ($Na_2O + K_2O$) extends towards ideal K-free nyerereite (Fig. 8) because the high K content reflects their overall composition as $(Na,K)_2Ca(CO_3)_2$. Similar Na–Ca carbonates occur as inclusions in magnetite from Kerimasi north slope calcite carbonatite (Fig. 8), which have been identified on the basis of Raman spectrometry by Zaitsev (2010) as *bona fide* nyerereite, although these are relatively poor in K_2O (1.6–1.9 wt.%) compared to the K-rich Na–Ca carbonates from Kerimasi afrikandite and nyerereite phenocrysts in Oldoinyo Lengai natrocarbonatites (Fig. 8). The Na–Ca carbonates from the Kerimasi afrikandite are thus the closest in composition to Oldoinyo Lengai nyerereite than any Na–Ca carbonate yet described from Kerimasi.

Secondary and supergene minerals

The interstitial and porous regions between calcite (C3) prisms, apart from apatite and spinel, are occupied principally by a wide variety of minerals which might have either secondary or supergene origins. The most abundant are gypsum and anhydrite occurring as veins and irregular patches which commonly include Ca–Mn–Fe oxide/hydroxides (Fig. 3). Gypsum, on the basis of textural relationships, appears to have been formed by hydration of anhydrite. Both anhydrite (58.4 SO_3; 41.5 CaO wt.%) and gypsum (46.4 SO_3; 33.4 CaO wt.%) have near-stoichiometric compositions.

Table 2. Representative compositions (wt.%) of monticellite.

Wt.%	1	2	3	4	5
SiO_2	37.44	37.34	37.56	36.99	37.53
CaO	37.06	34.90	34.79	36.04	35.59
MnO	1.54	2.31	2.74	3.10	4.10
FeO	1.68	1.66	1.25	1.42	1.71
MgO	23.17	23.59	22.79	21.29	21.77
Σ	100.89	99.80	99.13	99.34	100.70
Structural formula on the basis of O = 4 atoms per formula unit					
Si	0.986	0.993	1.003	0.994	0.996
Ca	1.046	0.992	0.996	1.038	1.012
Mn	0.034	0.052	0.062	0.071	0.093
Fe	0.037	0.037	0.028	0.032	0.038
Mg	0.910	0.933	0.90	0.873	0.866
Σ	3.013	3.007	2.997	3.008	3.005
Mg#	*96.09*	*96.20*	*97.02*	*90.47*	*95.78*
Mol.% end members					
Mon	92.73	91.32	90.98	89.50	86.87
Kir	3.77	3.60	2.80	3.27	3.83
Glc	3.50	5.08	6.22	7.23	9.30

Mon = monticellite $CaMgSiO_4$; Kir = kirschsteinite $CaFeSiO_4$; Glc = glaucochroite $CaMnSiO_4$

An unidentified hydrous Ca–Si–Mn–FeO oxide/hydroxide is common as small (<20 µm) ovoid particles included in anhydrite and as very fine grained material in the interstices between calcite laths. In some instances the larger examples exhibit minor very fine scale concentric compositional zonation suggestive of a colloidal origin (Fig. 3c). Regardless, the composition variation (wt.%) of several rastered areas is relatively constant: 19.7–19.9 FeO_T; 19.4–20.8 MnO; 9.24–10.5 CaO; 6.5–6.8 SiO_2; 1.7–1.8 BaO. Other common interstitial minerals are: baryte (58.7–60.9 BaO; 3.2–4.1 SrO; 1.6–2.4 CaO; 35.0–35.1 SO_3 wt.%); celestite (49.9 SrO; 6.2 CaO; 0.6; 0.6 BaO; 42.6 SO_3 wt.%) and strontianite (53.5–56.9 SrO; 4.0–6.4 CaO; 1.14 BaO, wt.%).

Discussion

The Trig Point Hill debris flow contains blocks of heterolithic pyroclastic carbonatite. Typically, these consist of three distinctive textural and mineralogical varieties of calcite carbonatite with 'corduroy' calcite (C1) and the calcite (C2) clasts with Na–Ca-carbonate inclusions, incorporated into a matrix of volcaniclastic prismatic calcite (C3) carbonatite. Similar carbonatites Fig. 9) are exposed at the crater rim (this work; Mariano and Roeder, 1983), within the pyroclastic deposits on the northern slopes of Kerimasi (Zaitsev, 2010), and at Tinderet volcano, Kenya (Zaitsev *et al.*, 2013). Hay (1983) proposed initially that the corduroy calcite (C1) clasts and the prismatic (C3) calcite laths are altered nyerereite. The only evidence for this supposition was that the textures of the rocks were similar to those of Oldoinyo Lengai natrocarbonatites, these being dominated by flow-aligned nyerereite prismatic crystals. The calcite (C2) clasts were considered as primary and to have crystallised before incorporation in 'natrocarbonatite', regardless that such calcite is not present at Oldoinyo Lengai. Hay (1983) did not recognise any Na–Ca-carbonates as inclusions in these calcites or that they are actually clasts in the calcite (C3) carbonatite matrix. The rocks described by Hay (1983) actually do not bear any textural resemblance to any fresh or altered Oldoinyo Lengai natrocarbonatite (Keller and Krafft, 1990; Peterson, 1990; Mitchell, 2006; Zaitsev *et al.*, 2008).

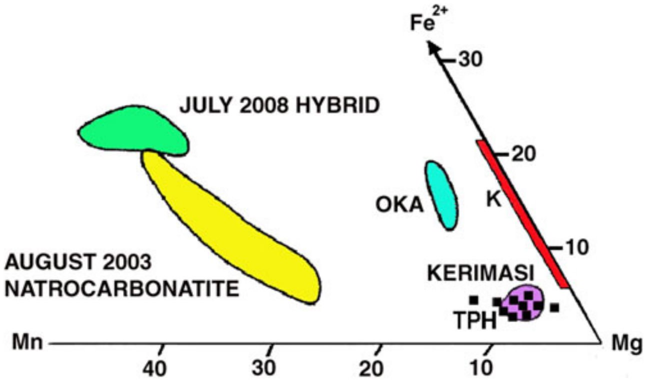

Fig. 5. Compositions of monticellite plotted in the ternary system Fe^{2+}–Mg–Mn (atoms per formula unit) from Trig Point Hill (TPH; black squares, this work) and Kerimasi (purple field from Mitchell and Belton, 2008), compared with monticellite from Oldoinyo Lengai natrocarbonatites erupted in 2003 and 2008, Oka calcite carbonatite and kimberlite (K) (Mitchell and Belton, 2008).

Hay (1983) did not describe any material which might be considered as altered gregoryite, nor was any recognised by us in this investigation. In contrast, Zaitsev (2010) has considered that 'corduroy' calcite (C1) clasts, referred to as 'banded calcite', from the north slope of Kerimasi are altered gregoryite. Zaitsev (2010) suggested that these clasts were initially gregoryite containing exsolved lamellae of nyerereite and that complete dissolution of gregoryite by meteoric water coupled with replacement of the nyerereite by calcite leads to the formation of the banded calcite clasts. However, Zaitsev (2010, p.638) also notes that "why and how banded crystalline segregations have formed remains unanswered". There is no mineralogical evidence that dolomite was involved in the formation of these segregations as suggested by Church (1995).

Zaitsev *et al.* (2013) have provided limited C and O isotopic data for Tinderet and Kerimasi clasts and shown that there are significant isotopic differences between primary prismatic C2 calcite and banded C1 calcite. What is apparent from these data is that there is a continuum between mantle-type compositions for C2 calcite and altered material (C1, C3) with high δ 18O(>+20‰). This is not surprising given that the C1 and C3 material is very porous and clearly has been subject to isotopic exchange with meteoric water. The formation of gypsum and other supergene minerals in these rocks attests to their extensive interaction with meteoric waters. In contrast, prismatic C2 is homogeneous and therefore less subject to such exchange. Regardless, isotopic equilibrium cannot be expected between any of these components and/or with meteoric water in their current environment. Consequently, stable isotopic studies are considered not to be informative regarding the genesis of these heterolithic pyroclastic rocks.

Other problems with this hypothesis are that none of the rocks actually have the textures of natrocarbonatites and the gregoryites at Oldoinyo Lengai are small (<1 mm), rounded-to-kidney shaped with common concentric zoning and mantling (Peterson, 1990; Keller and Krafft, 1990). These can in some instances contain 25–30 vol.% inclusions of nyerereite together with very fine grained exsolved nyerereite (Peterson, 1990). However, these modal volumetric relationships are the reverse of the corduroy clasts which are dominated by calcite. Thus, if a typical Lengai-type gregoryite were dissolved, a void would be created with concomitant collapse and aggregation of the unsupported

Table 3. Representative compositions of spinels from Trig Point Hill and Kerimasi crater.

Wt.%	1	2	3	4	5	6	7	8
MgO	8.10	11.83	13.12	12.31	10.21	5.11	5.91	6.77
Al_2O_3	3.25	8.92	5.57	4.50	3.67	1.04	1.25	2.02
TiO_2	12.77	3.60	1.12	n.d.	2.04	2.84	2.03	0.78
MnO	0.61	2.90	4.17	7.55	8.35	3.63	4.67	5.79
FeO_T	71.85	67.87	69.87	69.18	66.75	81.04	79.98	77.91
Σ	96.58	95.12	93.85	93.54	91.02	93.66	93.84	93.27
Fe_2O_3	45.68	58.85	67.84	70.84	66.75	65.19	66.99	68.92
FeO	30.74	14.91	8.83	5.43	9.61	22.39	19.40	15.89
Σ	101.15	100.61	100.65	100.63	100.64	100.20	100.25	100.17
Mol.% end-members								
$MgAl_2O_4$	6.67	16.82	11.08	9.05	7.51	2.25	2.68	4.30
$MgFe_2O_4$	35.80	42.25	54.93	53.61	45.34	25.69	29.40	32.14
$MnFe_2O_4$	1.80	8.23	11.92	21.83	24.56	11.27	14.40	17.70
Fe_2TiO_4	33.07	9.07	2.84	-	5.33	7.83	5.56	2.12
Fe_3O_4	22.66	23.63	19.23	15.51	17.26	52.96	47.96	43.74

Compositions: 1–5 Trig Point Hill spinels in the matrix of calcite (C3) prisms; 6–8 spinels in Kerimasi crater apatite carbonatite.
FeO_T = total Fe expressed as FeO; Fe_2O_3 and FeO calculated from total Fe on the basis of 24 cations and 32 atoms of oxygen by the method of Droop (1987).

nyerereite crystals, followed by their probable subsequent recrystallisation to anhedral aggregates of calcite without pseudomorphic replacement of any pre-existing textures. Zaitsev *et al.* (2008) have noted that alteration of natrocarbonatite at Oldoinyo Lengai leads to the complete elimination of gregoryite and only the rare formation of pirssonite pseudomorphs; observations not in accord with the gregoryite dissolution process described above as advocated by Zaitsev (2010) for the formation of corduroy calcite. In addition, Oldoinyo Lengai gregoryite contains significant amounts of phosphorus (1.3–4.5 wt.% P_2O_5; Peterson, 1990; Zaitsev *et al.*, 2009), which should be retained after dissolution as insoluble phosphates. These are not observed, nor are any of the major secondary minerals, i.e. pirssonite, kogargoite, formed during alteration of natrocarbonatite (Zaitsev *et al.*, 2008; Mitchell, 2006). Zaitsev (2010) has reported the presence of nyerereite from a Kerimasi north slope carbonatite, to support the existence of former natrocarbonatite. However, this nyerereite only occurs as inclusions in magnetite and its relevance to Hay's (1983) hypothesis is doubtful. Moreover, the composition of this nyerereite is very different to that of Lengai phenocrystal nyerereite (6–9 wt.% K_2O; Zaitsev *et al.*, 2009; Peterson, 1990) as it is poor in K_2O (1.6–1.9 wt.%).

The Na–Ca carbonate problem and natrocarbonatite volcanism

The presence of Na–Ca carbonates as micro-inclusions in a variety of calcite carbonatites at Kerimasi and elsewhere has, particularly recently, been construed as indicating an alkali-rich parental carbonatite magma which might differentiate to natrocarbonatite and even to common calcite carbonatite. Such a deduction is mistaken. Its advocates attribute absence of natrocarbonatite anywhere but at Oldoinyo Lengai as due to it having been dissolved during sub-aerial weathering. However, postulating a former presence from an assumed absence is not sound petrology. Moreover, it is evident that Na–Ca-inclusions in calcite at Kerimasi contain none of the characteristic minerals of *bona fide* natrocarbonatite, such as Ba-nyerereite, fluorite, khanneshite, halite–sylvite and cuspidine (Keller and Krafft, 1990; Peterson, 1990, Mitchell, 1997a, 2006; Mitchell and Belton, 2004). The parental melts to these inclusions crystallised calcite as a primary liquidus phase, and thus cannot differentiate to natrocarbonatite. Thus, the calcite has merely trapped deuteric Ca-Na-rich residual fluids/melts which have also crystallised apatite, monticellite, magnetite–jacobsite and perovskite – i.e. an undersaturated silicocarbothermal fluid/melt. Notably, monticellite and periclase are primary liquidus phases, and primary apatite is not stable in the Na–Ca–CO_2 residual fluids and is resorbed.

The 'altered nyerereite' problem

Flow-aligned calcite prisms are common in many calcite kimberlites, melilitites and carbonatites. Typical examples are: the Jos, Nikos and International kimberlites, Canada (Mitchell, 1997b); Kaiserstuhl lapilli tuffs, Germany (Keller, 1989);calcite carbonatite dyke rocks in the Guli and Maimecha-Kotui complexes, Siberia (Zhabin and Cherepivskaya, 1965; Zhabin, 1971); carbonatitic lavas at Catanda, Angola (Campeny *et al.*, 2015); Saltpetre Kop melilitites, South Africa (de Wit, 1975); and hypabyssal dykes at the Prairie Lake complex (this work). In all of these examples the textures are best considered as examples of rheological concentration of primary liquidus calcite as there are no petrographic indications that they might be pseudomorphs after some pre-existing phase. In particular, Campeny *et al.* (2015) have claimed, without any supporting evidence, that flow-aligned calcite found in clasts at Catanda are nyerereite pseudomorphs, regardless that the texture of these clasts is similar to that of primary calcite-bearing clasts occurring in Kaiserstuhl lapilli tuffs (Keller, 1989) and that these calcites exhibit compositional zoning. From these occurrences, and the experimental studies of Gittins and Jago (1991), demonstrating that calcite can crystallise at atmospheric pressure, there seems to be no *a priori* reason not to accept a primary origin for flow-aligned calcite-bearing carbonatites at Kerimasi, Homa, Tinderet, or Catanda (Deans and Roberts, 1984; Clarke and Roberts, 1986; Zaitsev *et al.*, 2013; Campeny *et al.*, 2015).

With respect to Tinderet, Le Bas (1984), in a discussion of the Deans and Roberts (1984) hypothesis, has noted that the flow-aligned calcite laths described are more probably altered melilite rather than nyerereite. This conclusion is supported by the brown alteration and texture as illustrated in fig. 3b of Deans and Roberts (1984), which is typical of altered melilite in many hypabyssal alnöites, okaites and melilitites (Larsen and Goransen 1932; Stansfield 1923; de Wit 1975; Hay 1978;

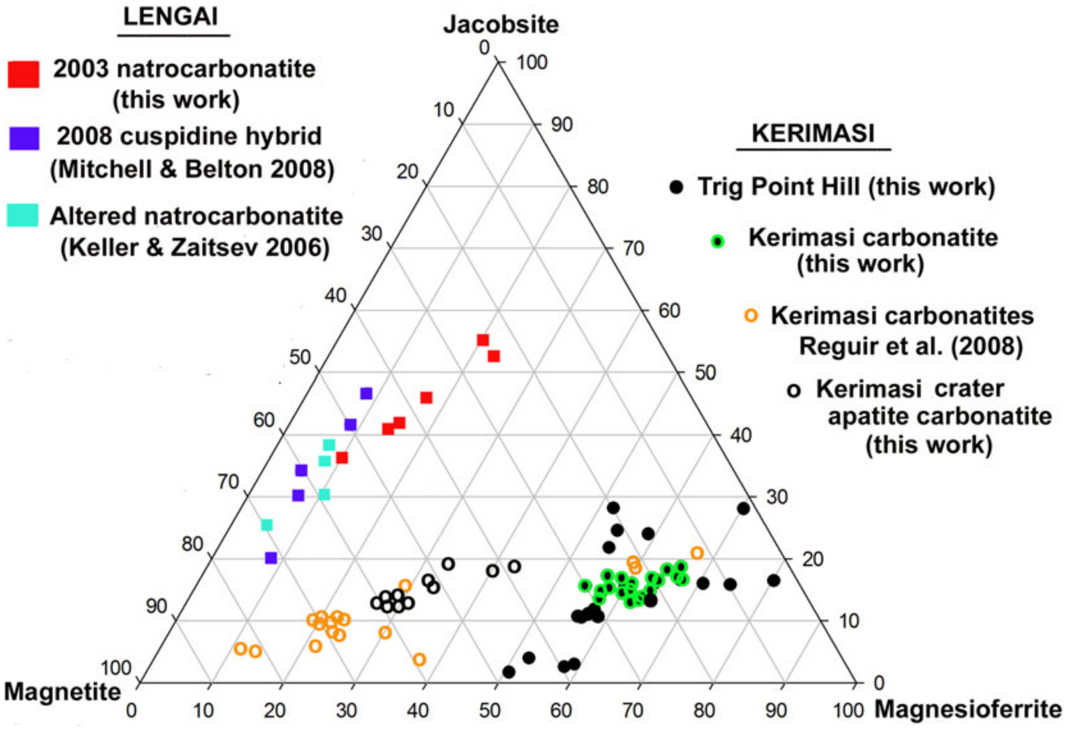

Fig. 6. Compositions of spinels plotted in the ternary system jacobsite–magnesioferrite–magnetite (mol.%), showing the pronounced dichotomy in composition between spinels from Oldoinyo Lengai natrocarbonatites belonging to the magnetite–jacobsite series versus those from Kerimasi calciocarbonatites which belong to the magnetite–magnesioferrite series.

Mitchell, 1997b; Zaitsev *et al.*, 2019). The alteration typically occurs under hydrothermal conditions and results in the formation of very fine grained cebollite, juanite and other hydrous Ca-silicates. Exact identification requires X-ray diffraction and/or Raman spectrometry.

Further evidence that flow-aligned calcite cannot be altered nyerereite is supported by preliminary analysis of length/breadth aspect ratios of prismatic melilite and calcite in melilitites and kimberlites as illustrated by: Mitchell (1997b); Keller and Zaitsev (2006); Peterson (1990); and Keller and Kraft (1990). Although, these data are not claimed here to be statistically rigorous they do suggest that random sections of orthorhombic prismatic nyerereite have different aspect ratios to those of rhombohedral calcite. At Nyiragongo (Zaire) and Armykon Hill (Tanzania) typical melilites have aspect ratios of 3.8–6.0 ($n = 15$: av. = 5.14) and 4.3–8.6 ($n = 10$; av. 6.7) respectively, and those of altered melilitite in an alnöite from Alnö (Sweden) are from 10–15 ($n = 5$). Calcite in the Jos kimberlite has aspect ratios ranging from 3.5–7 ($n = 8$; av. 5.1). In contrast, aspect ratios of *bona fide* altered nyerereite from Oldoinyo Lengai (Keller and Zaitsev, 2006) range from 2.1–5.5 ($n = 6$ av. 3.4), with those of fresh nyerereite illustrated by Peterson (1990) ranging from 2.3–5.2 ($n = 15$; av. 3.3). On the basis of these preliminary data it is considered as very unlikely that the Tinderet prismatic calcite illustrated in figs 3b–d of Deans and Roberts (1984) are altered nyerereite as they have aspect ratios of 5.7–12 ($n = 8$; av. 8.7). Further investigation of this topic is under consideration.

Table 4. Representative compositions of Na–Ca carbonates.

Wt.%	1	2	3	4	5	6	7	8	9	10
Na_2O	18.70	19.21	19.84	20.39	23.61	17.98	19.43	19.77	20.43	21.27
K_2O	1.70	1.97	2.44	2.53	2.37	2.70	2.55	5.83	6.20	5.97
CaO	32.01	33.00	31.96	31.11	27.94	33.43	32.88	27.04	27.54	27.96
SrO	0.59	1.03	0.69	0.46	0.37	0.39	0.50	0.69	0.60	0.87
SO_3	1.35	1.97	1.75	1.66	2.23	1.75	1.65	-	-	-
Σ	54.39	57.18	56.64	56.15	55.68	56.25	57.01	54.23	54.77	56.07
Recalc	93.79	98.08	97.28	96.42	96.48	96.68	99.65	91.61	93.19	96.28

Compositions|:1–5 Trig Point Hill; 6–7 Kerimasi north slope calcite carbonatite; 8–10 Kerimasi afrikandite. Recalc = Totals of Na,K,Ca,Sr contents recalculated as carbonate plus SO_3. Low totals reflect the presence of voids in the microcrystalline assemblage and not analytical errors.

Alteration of nyerereite to calcite has been shown by Zaitsev and Keller (2006) to proceed in three stages: (1) hydration of nyerereite to form pirssonite [($Na_2Ca(CO_3)·2H_2O$]; (2) leaching of Na from pirssonite; (3) dehydration of pirssonite to calcite (± shortite).These process must involve both dissolution and precipitation reactions (Putnis and Austrheim, 2010) and involve very significant density and volume changes as reaction (1) requires a molar volume increase from 81.10 cm^3 to 103.02 cm^3 followed by Na and H_2O loss, Ca 'solution' and redeposition as denser calcite with a lower molar volume (36.92 cm^3). It seems extremely unlikely that such processes can produce isovolume pseudomorphic replacement of nyerereite as the volume increase incurred during pirssonite formation would, on decomposition of this phase, result in the formation of significant voids or porosity such as are evident in figure 2 of Zaitsev *et al.* (2008) and figures 5 and 6 of Keller and Zaitsev (2006).

Although it is possible to devise theoretical isovolume replacement compositional reactions (Keller and Zaitsev, 2006) for the transformation of nyerereite via pirssonite and gaylussite to calcite there are no grounds for assuming that the transformations as proposed in these reactions is thermodynamically possible or is valid in the actual alteration environment. In particular, these

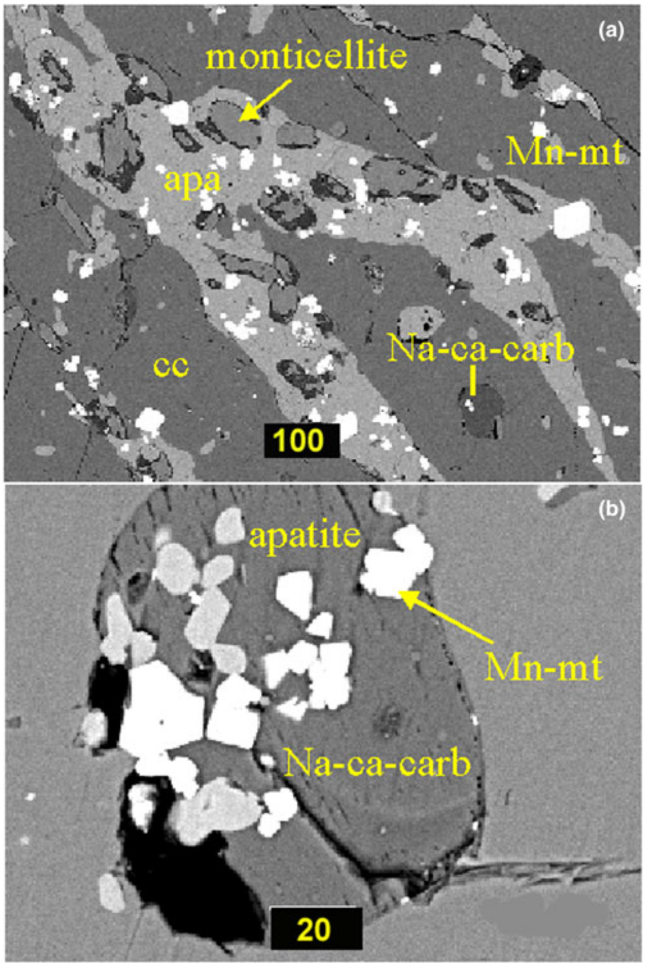

Fig. 7. Back-scattered electron images of calciocarbonatites from the north slope of Kerimasi. (a) Veins of apatite, monticellite and magnetite–magnesioferrite in calcite (cc) with inclusions of Na–Ca carbonate; and (b) Inclusion of Na–Ca carbonate in calcite with anhedral apatite and subhedral magnetite–magnesioferrite.

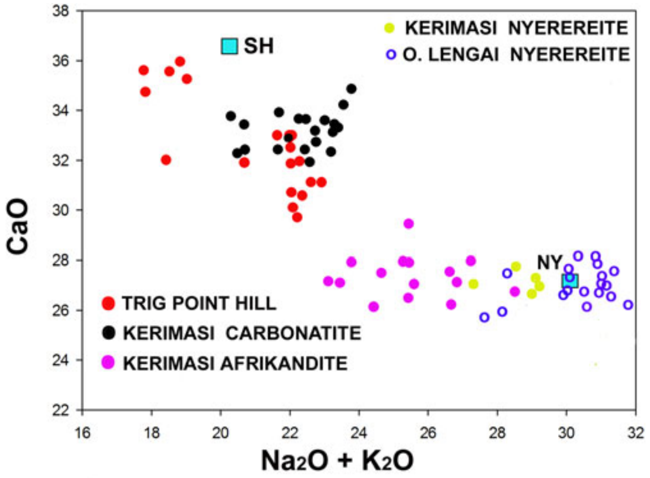

Fig. 8. Compositions (wt.%) of alkali carbonates occurring as inclusions in calcite from Trig Point Hill calcite (C2), Kerimasi calcite carbonatite, and afrikandite (this work), compared with the compositions of Oldoinyo Lengai nyerereite (Zaitsev *et al.*, 2009) and Kerimasi nyerereite (Zaitsev, 2010) SH = shortite; NY = ideal K-free nyerereite.

isovolume replacement equations neglect the role of other elements (Ca, K, Na, S and Cl) being added to the pseudomorphing fluids by the simultaneous decomposition of associated minerals such as gregoryite and halite–sylvite solid solutions. The latter are highly soluble in meteoric water and although NaCl does not hydrolyse, further Na will be added to the pseudomorphing fluids. In contrast, the hydrolytic solution of KCl will result in an increase in acidity and further promote Na–Ca-carbonate dissolution. For example the pH of a 3 m\l KCl solution in H_2O at 20°C is 6.2.

Keller and Zaitsev (2006) suggest that nyerereite replacement does not require an external source of Ca and that sufficient Ca is liberated during the decomposition process to form the calcite pseudomorphs. However, it is not evident that any Ca liberated would be sufficient to fill the solution void. As noted above it is extremely unlikely that the fluids involved in any replacement are pure water but rather will be solutions which might be saturated with diverse salts. If this happened to be calcium carbonate then even a small amount of dissolution of nyerereite would supersaturate the interfacial fluids and calcite or amorphous $CaCO_3$ or granular calcite might be expected to be precipitated, as shown in figure 7 of Zaitsev *et al.* (2008). However, if the dissolution rate was faster than the precipitation rate, the dissolution–precipitation reaction would become decoupled and no pseudomorphism would occur (Putnis and Austrheim 2010).

These observations are in accord with the conclusions of Putnis and Mezger (2004) and Putnis and Austrheim (2010) that pseudomorphing by dissolution–precipitation reactions can be very complex but typically result in the development of porosity. It is considered here that complete pseudomorphing of nyerereite by calcite would require the addition of calcium from externally-derived acidic fluids, followed by recrystallisation as a single crystal with the original habit of the nyerereite and well-developed porosity. Such porosity is not evident in any of the calcite considered to be pseudomorphs. From the above discussion it is evident that replacing nyerereite with calcite as perfect pseudomorphs is not a viable hypothesis.

Natrocarbonatite

It is apparent that the formation of natrocarbonatite at Oldoinyo Lengai is associated with undersaturated silicate volcanic rocks such as combeite wollastonite nephelinite (Mitchell and Dawson, 2012); an observation supported by experimental studies of synthetic carbonate-bearing silicate systems (Kjarsgaard *et al.*, 1995). The presence of a K-rich nyerereite-like mineral in association with peralkaline silicate glass as inclusions in perovskite and magnetite in Kerimasi afrikandite (this work; Guzmics *et al.*, 2012), and Na–Ca-carbonates as inclusions in minerals of the Gardiner, Kovdor and Guli carbonatites (Veksler *et al.*, 1998; Kogarko *et al.*, 1991) supports an association with melilite-crystallising magmas rather than nephelinite/phonolitic magmas. These observations suggest that peralkalinity in sodic magmas is a prerequisite for natrocarbonatite formation and that the process requires extreme differentiation together with immiscibility between sodic peralkaline and carbonate melts (Mitchell and Dawson, 2012; Kjarsgaard *et al.*, 1995; Guzmics *et al.*, 2012; Kaldos *et al.*, 2015).

Volcanoes such as Kerimasi, which are characterised by melilite-nephelinite magmatism might indeed have produced a variety of natrocarbonatite at some stage in their evolution during

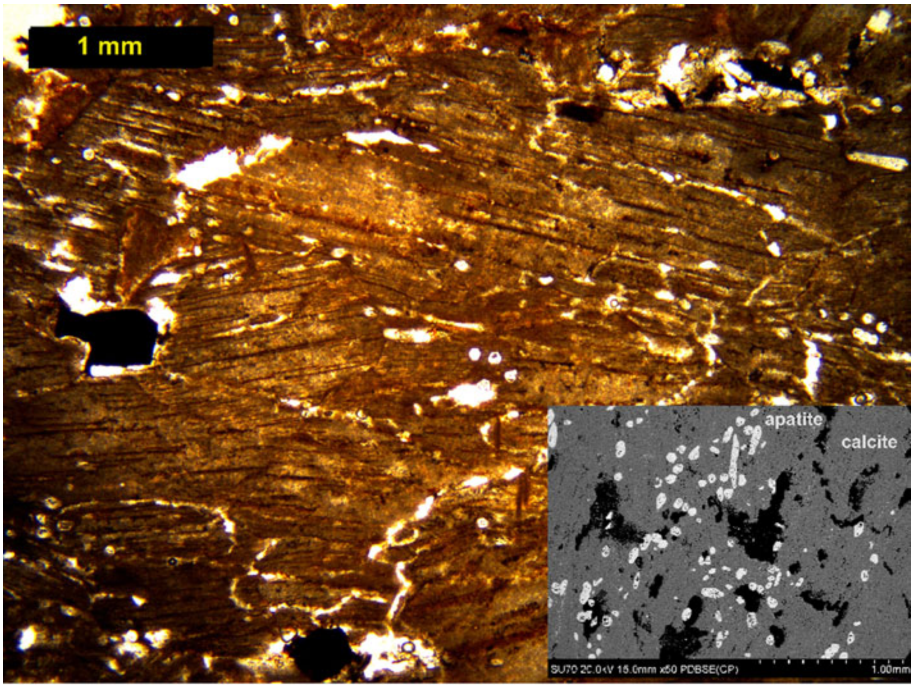

Fig. 9. Altered calciocarbonatite tephra from the rim of the current crater at Kerimasi consisting of flow-aligned calcite prisms and colourless subhedral-to-round microphenocrysts of apatite. The inset is a back-scattered electron image illustrating the abundance of apatite in this carbonatite.

the formation of the melilite-pyroxenites (afrikandites) within the roots of the volcano. Unfortunately there is no actual evidence for their existence at the current level of erosion and extrapolation of small inclusions to significant volumes of 'natrocarbonatite' is neither desirable nor warranted. Regardless, is it considered that the magmas which give rise to calcite carbonatites either as effusive or intrusive rocks will not differentiate to natrocarbonatites nor are natrocarbonatites precursors to calcite carbonatites. Typically one can expect the latter to be formed from the differentiation of carbonated melilititic or nephelinitic magmas with the formation of calcite cumulates and alkali enriched carbohydrothermal residua (Mitchell, 2005).

In summary, the Trig Point Hill and Kerimasi crater rim carbonatites cannot be an altered natrocarbonatite as: (1) the deposits are a heterolithic breccia; (2) there is no textural or compositional evidence to suggest that any of the prismatic calcite laths are altered nyerereite (see below); (3) spinels and monticellite are poor in Mn (Figs 5 and 6) relative to these minerals in Oldoinyo Lengai natrocarbonatites; (4) fluorite, which can be expected to be a stable relict phase in altered natrocarbonatite is a very rare mineral in the Trig Point Hills rocks; and when present does not exhibit the characteristic texture of groundmass fluorite in natrocarbonatite.

A further conclusion of the above discussion is that flow-aligned calcite in extrusive calcite carbonatites is either a primary liquidus mineral or altered melilite. To use the replacement concept to imply that natrocarbonatite might be relatively common is completely unwarranted and misleading.

Acknowledgements. This work is presented as a memorial to the late John Barry Dawson (1932–2013) who introduced me to the exotic rocks of Oldoinyo Lengai and Kerimasi. This investigation was initiated subsequent to our last visit to Trig Point Hill but was unfortunately interrupted by Barry's untimely passing. This study has been supported by the Natural Sciences and Engineering Council of Canada, Lakehead University and Almaz Petrology. Dorobo Safaris of Arusha (Tanzania) are thanked for logistical support at Kerimasi and Oldoinyo Lengai. Valerie Dennison is thanked for editorial assistance. Anatoly Zaitsev and two anonymous reviewers are thanked for editorial and scientific comments.

References

Bailey D.K. (1993) Carbonatite magmas. *Journal of the Geological Society, London*, **150**, 637–651.

Campeny M., Kamenetsky V.S., Melgarejo J.C., Mangas J., Manuel J., Alfonso P., Kamenetsky M.B., Bambi A.C.J.M. and Gonçalves A.O. (2015) Carbonatitic lavas in Catanda (Kwanza Sul, Angola): Mineralogical and geochemical constraints on the parental melt. *Lithos*, **232**, 1–11.

Church A.A. (1995) *The Petrology of the Kerimasi Carbonatite Volcano and the Carbonatites of Oldoinyo Lengai with a Review of Other Occurrences of Extrusive Carbonatites*. Unpublished PhD thesis, University of London, London, UK, 384 pp.

Clarke M.G.C. and Roberts B. (1986) Carbonated melilitites and calcitized alkali carbonatites from Homa Mountain, western Kenya: a reinterpretation. *Geological Magazine*, **123**, 683–692.

Dawson J.B. (2008) *The Gregory Rift Valley and Neogene-Recent Volcanoes of Northern Tanzania*. Memoir of the Geological Society of London, **33**. The Geological Society, London (UK), 102 pp.

Dawson J.B., Garson M.S. and Roberts D. (1987) Altered former alkalic carbonatite lava from Oldoinyo Lengai, Tanzania inferences for calcite carbonatite lavas. *Geology*, **15**, 765–768.

Deans T.D. and Roberts B. (1984) Carbonatite tuffs and lava clasts of the Tinderet foothills, western Kenya: a study of calcified natrocarbonatites. *Journal of the Geological Society, London*, **141**, 563–580.

Delcamp A., Delvaux D., Kwela G., Mocheyek A. and Kervyn M. (2016) Sector collapse events at volcanoes in the North Tanzanian divergence zone and their implications for regional tectonics. *Geological Society of America Bulletin*, **128**, 169–186.

de Wit J.J. (1975) Carbonatites and related rocks at Saltpetre Kop, Sutherland, Cape Province. *Annals of the University of Stellenbosch Series A1 (Geology)*, **1**, 193–232.

Droop G.T.R. (1987) A general equation for estimating Fe^{3+} concentrations in ferromagnesian silicates and oxides from microprobe analyses, using stoichiometric criteria. *Mineralogical Magazine*, **51**, 431–435.

Gittins J. and Harmer R.E. (1997) Dawson's Oldoinyo Lengai calciocarbonatite: a magmatic sövite or an extremely altered natrocarbonatite? *Mineralogical Magazine*, **61**, 351–355.

Gittins J. and Jago B.C. (1991) Extrusive carbonatites: their origins reappraised in the light of new experimental data. *Geological Magazine*, **128**, 301–305.

Guest N.J. (1953) *The Geology of Part of Northern Tanganyika Territory*. Unpublished PhD Thesis, University of Sheffield, UK.

Guzmics T., Mitchell R.H, Szabo C., Berkesi M., Milke R. and Abart R. (2011) Carbonatite melt inclusions in coexisting magnetite apatite and monticellite in Kerimasi calciocarbonatite, Tanzania: melt evolution and petrogenesis. *Contributions to Mineralogy and Petrology*, **161**, 177–196.

Guzmics T., Mitchell R.H., Szabo C., Berkesi M., Milke R. and Ratter K. (2012) Liquid immiscibility between silicate, carbonate and sulfide melts in melt inclusions hosted in co-precipitated minerals from Kerimasi volcano (Tanzania) evolution of carbonated nephelinitic magma. *Contributions to Mineralogy and Petrology*, **164**, 101–122.

Hay R.L. (1978) Melilitite-carbonatite tuffs in the Laetolil beds of Tanzania. *Contributions to Mineralogy and Petrology*, **67**, 357–367.

Hay R.L. (1983) Natrocarbonatite tephra of Kerimasi volcano, Tanzania. *Geology*, **11**, 599–602.

Káldos Guzmics T., Mitchell Dawson J.B., Milke R. and Szabo C. (2015) A melt evolution model for Kerimasi volcano, Tanzania: Evidence from carbonate melt inclusions in jacupirangite, *Lithos*, **238**, 101–119.

Keller J. (1989) Extrusive carbonatites and their significance: Pp. 70–88 in: *Carbonatites – Genesis and Evolution* (K. Bell, editor). Unwin Hyman, London, UK.

Keller J. and Krafft M. (1990) Effusive natrocarbonatite activity of Oldoinyo Lengai, June 1988. *Bulletin of Volcanology*, **52**, 629–645.

Keller J. and Zaitsev A.N. (2006) Calciocarbonatite dykes at Oldoinyo Lengai, Tanzania: the fate of natrocarbonatite. *The Canadian Mineralogist*, **44**, 857–876.

Kervyn M., Ernst G.G., Klaudius J., Keller J., Mbedes E. and Jacobs P. (2008) Remote sensing study of sector collapse and debris avalanche deposits at Oldoinyo Lengai and Kerimasi volcanoes, Tanzania. *Journal of Remote Sensing*, **29**, 6565–6595.

Kjarsgaard B.A., Hamilton D.L. and Peterson T.D. (1995) Peralkaline nephelinite/carbonatite liquid immiscibility: comparison of phase compositions in experiments and natural lavas from Oldoinyo Lengai. Pp. 163–190 in: *Carbonatite Volcanism* (K. Bell and J. Keller, editors). Springer-Verlag, Berlin.

Kogarko L.N., Plant D.A., Henderson C.M.B. and Kjarsgaard B.A. (1991) Na-rich carbonate inclusions in perovskite and calzirtite from the Guli intrusive carbonatite, polar Siberia. *Contributions to Mineralogy and Petrology*, **109**, 124–129.

Le Bas M.J. (1984) Discussion of Deans and Roberts, *vide supra*. *Journal of the Geological Society*, **141**, 580.

Larsen E.S. and Goransen E.A. (1932) The deuteric and later alteration of the uncomphagrite of Iron Hill, Colorado. *American Mineralogist*, **17**, 343–356.

Mariano A.N. and Roeder P.L (1983) Kerimasi: a neglected carbonatite volcano. *Journal of Geology*, **91**, 449–455.

Mattson H.B. (2012) Rapid magma ascent and short eruption durations in the Lake Natron-Engaruka monogenetic volcanic field (Tanzania): a case study of the olivine melilititic Pello Hill scoria cone. *Journal of Volcanology and Geothermal Research*, **247–248**, 16–25.

Mitchell R.H. (1997a) Carbonate-carbonate immiscibility, neighborite, and potassium iron sulphide in Oldoinyo Lengai natrocarbonatite. *Mineralogical Magazine*, **61**, 779–789.

Mitchell R.H. (1997b) *Kimberlites, Orangeites, Lamproites, Melilitites, and Minettes: A Petrographic Atlas*. Almaz Press, Thunder Bay, Ontario, Canada (www.almazpress.com)

Mitchell R.H. (2005) Carbonatites and carbonatites and carbonatites. *The Canadian Mineralogist*, **43**, 2049–2068.

Mitchell R.H. (2006) Sylvite and fluorite microcrysts, and fluorite-nyerereite intergrowths from natrocarbonatite, Oldoinyo Lengai, Tanzania. *Mineralogical Magazine*, **70**, 101–114.

Mitchell R.H. and Belton F.A. (2004) Niocalite–cuspidine solid solution and manganoan monticellite from natrocarbonatite, Oldoinyo Lengai, Tanzania. *Mineralogical Magazine*, **68**, 787–799.

Mitchell R.H. and Belton F.A. (2008) Cuspidine-sodalite natrocarbonatite from Oldoinyo Lengai, Tanzania: a novel hybrid natrocarbonatite formed by the assimilation of ijolite. *Mineralogical Magazine*, **72**, 1147–1162.

Mitchell R.H. and Dawson J.B. (2012) Carbonate-silicate immiscibility and extremely peralkaline glasses from Nasira cone and recent eruptions at Oldoinyo Lengai Volcano, Tanzania. *Lithos*, **152**, 40–46.

Peterson T.D. (1990) Petrology and genesis of natrocarbonatite. *Contributions to Mineralogy and Petrology*, **105**, 143–155.

Putnis A. and Austrheim H. (2010) Fluid-induced processes: metasomatism and metamorphism. *Geofluids*, **10**, 254–269.

Putnis C. and Mezger K. (2004) A mechanism of mineral replacement: Isotope tracing in the model system KCl–KBr–H_2O. *Geochimica et Cosmochimica Acta*, **68**, 2839–2848.

Reguir E.P., Chakhmouradian A.R., Halden N.M., Yang P. and Zaitsev A.N. (2008) Early magmatic and reaction-induced trends in magnetite from the carbonatites of Kerimasi, Tanzania. *The Canadian Mineralogist*, **46**, 879–900.

Stansfield J. (1923) Extensions of the Monteregian petrographical province to the west and northwest. *Geological Magazine*, **60**, 433–453

Stoppa F., Schiazza M., Rosatelli G., Castorina F., Sharygin V.V., Ambrosioa F.A. and Vicentinia N. (2019) Italian carbonatite system: From mantle to ore-deposit. *Ore Geology Reviews*, **114**, 103141.

Treiman AH. and Essene E.J. (1984) A periclase-dolomite-calcite carbonatite from the Oka complex, Quebec and its calculated volatile composition. *Contributions to Mineralogy and Petrology*, **85**, 149–157.

Veksler I.V., Nielsen T.F.D. and Sokolov S.V. (1998) Mineralogy of crystallized melt inclusions from Gardiner and Kovdor ultramafic alkaline complexes: implications for carbonatite genesis. *Journal of Petrology*, **39**, 2015–2031.

Woolley A.R. and Church A.A. (2005) Extrusive carbonatites: a brief review. *Lithos*, **85**, 1–14.

Zaitsev A.N. (2010) Nyerereite from calcite carbonatite at the Kerimasi volcano, northern Tanzania. *Geology of Ore Deposits*, **52**, 630–640.

Zaitsev A.N. and Keller J. (2006) Mineralogical and chemical transformation of Oldoinyo Lengai natrocarbonatites, Tanzania. *Lithos*, **91**, 191–207.

Zaitsev A.N, Keller J. and Billström K. (2009) Isotopic composition of Sr, Nd, and Pb in pirssonite, shortite and calcite carbonatites from Oldoinyo Lengai volcano, Tanzania. *Doklady Earth Sciences*, **425**, 302–306.

Zaitsev A.N, Keller J., Sprat J., Perova E.N. and Kearsley A. (2008) Nyerereite - pirssonite - calcite -shortite relationships in altered natrocarbonatites. Oldoinyo Lengai, Tanzania. *The Canadian Mineralogist*, **46**, 843–860.

Zaitsev A.N., Keller J., Spratt J., Jeffries T.E. and Sharykin V.V. (2009) Chemical composition of nyerereite and gregoryite from natrocarbonatites of Oldoinyo Lengai volcano, Tanzania. *Geology of Ore Deposits*, **51**, 608–616

Zaitsev A.N., Wenzl T., Venneman T. and Markl G. (2013) Tinderet volcano, Kenya: an altered natrocarbonatite locality? *Mineralogical Magazine*, **77**, 213–226.

Zaitsev A.N., McHenry L., Savchenok A.I., Strekopytov S., Spratt J., Humphreys-Williams E., Sharygin V.V., Bogomolov E.S., Chakhmouradian A.R., Zaitseva O.A., Arzamastsev A.A., Reguir E.P., Leach L., Leach M. and Mwankunda J. (2019) Stratigraphy, mineralogy and geochemistry of the Upper Laetolil tuffs including a new tuff 7 site with footprints of Australopithecus afarensis, Laetolil, Tanzania. *Journal of African Earth Sciences*, **158**, 103561.

Zhabin A.G. (1971) Primary textural-structural features of carbonatites and their metamorphic evolution. *International Geology Review*, **13**, 1087–1096.

Zhabin A.G. and Cherepivskaya G.Y. (1965) Carbonatite dikes as related to ultrabasic-alkalic extrusive activity. *Doklady Akademiya Nauk SSSR, Earth Sciences Section*, **160**, 135–138.